Title

Characterization of natural organic matter in low-carbon sediments: Extraction and analytical approaches

Authors

Fox, Patricia M
Nico, Peter S
Tfaily, Malak M
et al.

Publication Date

2017-12-01

DOI

10.1016/j.orggeochem.2017.08.009

Peer reviewed

Characterization of natural organic matter in low-carbon sediments: Extraction and analytical approaches

Patricia M. Fox[a] Peter S. Nico[a] Malak M. Tfaily[b] Katherine Heckman[c] James A. Davis[a]

Abstract

Organic carbon (OC) concentrations in subsurface sediments are typically 10 to 200 times lower than in surface soils, posing a distinct challenge for characterization. In this study, a range of chemical extractions were evaluated for extraction of natural organic matter (NOM) from two low-carbon (< 0.2%) alluvial sediments. The OC extraction efficiency followed the order pyrophosphate (PP) > NaOH > HCl, hydroxylamine hydrochloride > dithionite, water. A NOM extraction and purification scheme was developed using sequential extraction with water (MQ) and sodium pyrophosphate at pH 10 (PP), combined with purification by dialysis and solid phase extraction in order to isolate different fractions of sediment-associated NOM. Characterization of these pools of NOM for metal content and by Fourier transform infrared spectroscopy (FITR) showed that the water soluble fraction (MQ-SPE) had a higher fraction of aliphatic and carboxylic groups, while the PP-extractable NOM (PP-SPE and PP > 1kD) had higher fractions of CC groups and higher residual metals. This trend from aliphatic to more aromatic is also supported by the specific UV absorbance at 254 nm ($SUVA_{254}$) (3.5 vs 5.4 for MQ-SPE and PP-SPE, respectively) and electrospray ionization Fourier transform ion cyclotron resonance spectrometry (ESI-FTICR-MS) data which showed a greater abundance of peaks in the low O/C and high H/C region (0–0.4 O/C, 0.8–2.0 H/C) for the MQ-SPE fraction of NOM. Radiocarbon measurements yielded standard radiocarbon ages of 1020, 3095, and 9360 years BP for PP-SPE, PP > 1kD, and residual (non-extractable) OC fractions, indicating an increase in NOM stability correlated with greater metal complexation, apparent molecular weight, and aromaticity.

Graphical abstract

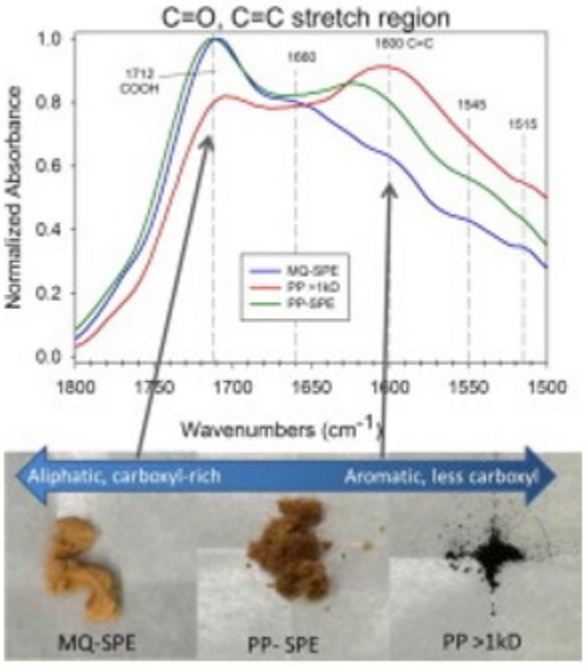

Keywords: Natural organic matter, Soil, Sediment, Chemical extraction, Chemical characterization, FTIR, ESI-FTICR-MS

1. Introduction

Belowground stocks of carbon (*i.e.*, in soils & sediments) represent a large fraction of the total earth carbon stocks, storing more than twice the carbon than the atmosphere and living plants combined (Fischlin et al., 2007). Despite decreasing organic carbon (OC) concentrations with depth in soils, approximately half of the soil carbon may be stored in the deeper subsurface (> 1 m) (Trumbore et al., 1995). It is largely unknown how subsurface carbon will respond to climate change (Conen et al., 2006, Smith et al., 2008, Conant et al., 2011, Rumpel and Kögel-Knabner, 2011;). Given the large size of this pool of carbon, research on the chemical nature of soil or sediment organic carbon and the factors controlling its stability is critical in order to understand and predict the dynamics of this pool.

For surface soils containing relatively high (5–10%) levels of OC, direct *in situ* analysis of natural organic matter (NOM) by FTIR (*e.g.*, Kaiser et al., 2016), synchrotron-based techniques (STXM, NEXAFS, FTIR) (*e.g.*, Lehmann et al., 2007, Remusat et al., 2012), and CPMAS NMR (*e.g.*, Kögel-Knabner, 2000, Knicker et al., 2006) are possible. Destructive techniques, such as pyrolysis GC–MS and thermal analysis are also applied to soils (*e.g.*, Plante et al., 2009, de la Rosa et al., 2011, González-Pérez et al., 2014), although interpretation of these data sets are more complex due to the alterations to OC structure during analysis. However, in low OC (< 1%) soils or sediments, such as those in the deeper subsurface (> 1 m), many of these techniques are not sensitive enough to be applied directly to the bulk material, necessitating the use of extractions to separate NOM from the mineral

components. Extraction allows for the characterization of different pools of NOM with presumably different mobilization potentials and reactivities, potentially providing more information on NOM association and stability compared to bulk analytical techniques. For example, many studies have characterized the water-soluble NOM fraction of soils (*e.g.,*Ellerbrock and Kaiser, 2005, Kaiser and Ellerbrock, 2005, Heckman et al., 2011, Ohno et al., 2014, Kaiser et al., 2016). Separation and characterization of so-called "humic" and "fulvic" acid fractions is also common (*e.g.,*Solomon et al., 2005, Ikeya et al., 2012, Ikeya et al., 2015, DiDonato et al., 2016), based on their solubility in acidic and alkaline solutions (Stevenson, 1994). Recently, Tfaily et al. (2015) investigated a range of organic solvents to extract soil OM and characterized the extracted fractions using ESI-FTICR-MS. Due to observations of the correlation between metals (Fe, Al) and OC in natural waters and soils (Kaiser and Guggenberger, 2000, Knorr, 2013), a number of extractions have been employed to extract "Fe- and Al-associated" soil OM. These include alkaline sodium pyrophosphate (*e.g.*, Ellerbrock and Kaiser, 2005, Kaiser and Ellerbrock, 2005, Kaiser et al., 2016), which targets OM bound to mineral surfaces via ligand exchange and cation bridging as well as OM in metal-OM complexes, and dithionite (Wagai and Mayer, 2007, Lalonde et al., 2012, Wagai et al., 2013), which targets OM bound to crystalline Fe-oxides and oxyhydroxides. Sequential extraction schemes of varying degrees of complexity which include many of the extractants discussed above have also been developed to extract different pools of mineral-bound NOM (*e.g.*, Posner, 1966, Lopez-Sangil and Rovira, 2013).

The goals of this study were to (1) evaluate extraction approaches to separate soil NOM from mineral components and develop an extraction and isolation approach for understudied low-carbon sediments, (2) characterize the different extracted NOM pools using FTIR and ESI-FTICR-MS, and (3) provide insight into the stabilization mechanisms of NOM in low-carbon sediments. By developing this protocol, we hope to facilitate more investigations into the chemical nature of organic carbon in low carbon sediments and alleviate a potential bias that could result from only high-OC materials being considered for analysis.

2. Materials and methods

2.1. Site description and sediment samples

Two sediment samples [Little Rusty Composite (LRC) and Backhoe 2-1-13 (BH)] were collected from a subsurface alluvial aquifer in Rifle, Colorado hosted within a floodplainalong the Colorado River. The shallow, unconfined aquifer has a saturated thickness of approximately 4 m, and is underlain by the impermeable Wasatch formation at approximately 8 m below ground surface (DOE, 1999, Yabusaki et al., 2007). The aquifer sediment consists of unconsolidated clay, silt, sand, gravel and cobbles, with approximately 30% of sediment in the < 2 mm fraction (DOE, 1999, Fox et al., 2012).

Sediment mineralogy is primarily composed of quartz and feldspars, with minor amounts of calcite, chlorite, kaolinite and iron oxides (magnetite, hematite, and goethite) (Komlos et al., 2008, Campbell et al., 2012, Fox et al., 2013). A description of the LRC sediment sampling and processing is provided by Hyun et al. (2009). Briefly, the sample was collected by backhoe from just below the water table (approximately 4.6 m below ground surface), air-dried for approximately 1 week, and sieved to < 2 mm. BH sediment was collected in a similar manner on February 1, 2013. However, the BH sample was not air-dried, but was sieved to < 2 mm under field-moist conditions and stored at 4 °C. Very little visible litter fragments (roots, twigs, etc.) were present in these samples, thus it is expected that the vast majority of the organic carbon in these sediments resides in the < 2 mm size fraction. The water content of BH was determined by drying a subsample at room temperature and all data are presented in terms of dry weight of sediment.

2.2. Extractions

2.2.1. Single extractions

Sediments were subjected to six different extractions, designed to target various mineralogical (*e.g.*, Fe-oxide/oxyhydroxide) and organic pools as shown in Table 1. All extractions were carbon-free in order to allow for analysis of extracted OC. The acidic extracts HCl and hydroxylamine hydrochloride (HH) are designed to dissolve amorphous or easily reducible Fe-oxides (Chao and Zhou, 1983) and NOM associated with those minerals. However, these extracts will only release NOM which is soluble at acidic pH. The inorganic dithionite extraction targets NOM associated with both crystalline and non-crystalline Fe-oxides (Wagai and Mayer, 2007), and includes a dilute HCl rinse to release any FeS precipitated in the dithionite solution. Alkaline extracts are often more effective at releasing NOM from soils, thus we also test NaOH, an extractant commonly used to extract NOM (Stevenson, 1994) and sodium pyrophosphate (PP), which in addition to the alkaline pH has metal-chelating properties which can solubilize NOM stabilized through metal complexation (Loeppert and Inskeep, 1996, Pansu and Gautheyrou, 2006).

Table 1. Chemical extractions applied to sediment samples.

Extraction	**Target pool**	**Method**	**Reference**
MQ	Water-soluble OM	MilliQ water, 20 h, 200 g/L	
PP	OM−complexed Fe	0.1 M sodium pyrophosphate, pH 10, 20 h,	Loeppert and Inskeep

Extraction	Target pool	Method	Reference
		200 g/L	(1996)
HCl	Amorphous Fe-oxide bound OM	0.5 M HCl, 1 h, 200 g/L	
HH	Easily reducible Fe and Mn-bound OM	0.25 M hydroxylamine hydrochloride, 0.25 M HCl, 50 °C, 1 h, 200 g/L	Chao and Zhou (1983)
Dithionite	Iron-oxide bound OM	100 g/L dithionite, 16 h; followed by 0.05 M HCl rinse 1 h; 167 g/L	Wagai and Mayer (2007)
NaOH	Humic and fulvic acids	0.5 M NaOH, 20 h, 200 g/L	Stevenson (1994)

Each extraction was performed at least in triplicate and results are presented as the average and standard deviation of the replicates. For each extraction, 5 g sediment was weighed into 50 mL polycarbonate centrifuge tubes, extractant was added, and tubes were capped and placed on an end-over-end sample rotator for the specified time, except for HH extractions, which were performed at 50 °C in a shaking water bath. Samples were then centrifuged at 25,000*g* for 30 min and the supernatant was filtered through a 0.45 µm (PVDF or Acrodisc Supor PES) syringe filter. Method blanks were produced for each extractant using only the extracting solution (*i.e.*, without solid); these blanks were processed and analyzed in the same manner as the samples. The pyrophosphate and dithionite extractions were tested at several different solid to liquid ratios (10–200 g/L for PP and 33–167 g/L for dithionite). Results from the solid to liquid ratio tests are shown in the supporting information (SI).

2.2.2. Sequential extractions

Based on the results of the single extractions, a sequential extraction protocol was developed using water (MQ) and sodium pyrophosphate (PP) on larger sediment samples in order to recover enough NOM for FTIR and ESI-FTICR-MS analysis. The extraction parameters

remained the same, but 40 g sediment samples were used with 200 mL of extracting solution in a 300 mL polycarbonate bottle and extractions were mixed on an orbital shaker table. After the MQ extraction, the sediment was allowed to settle and the liquid was poured off into a 250 mL polycarbonate centrifuge bottle, centrifuged at 25,000*g* and filtered through a 0.45 µm Acrodisc Supor PES syringe filter. The sediment remaining in the centrifuge bottle was then transferred back to the original extraction bottle using 200 mL of PP extractant, and weighed to determine the total solution volume. PP extracts were centrifuged and filtered in the same manner as the MQ extracts.

2.3. NOM concentration and purification

High levels of salts and metals, particularly in the PP extracts, severely interfere with analysis of extracted NOM. Low NOM concentrations in the MQ-extracted fraction also limit analysis, necessitating concentration and purification of the extracted NOM prior to analysis. Therefore, sequentially extracted MQ and PP extracts were treated using a combination of solid-phase extraction (SPE) and dialysis in order to concentrate the NOM and remove salts and metals to allow for analysis by FTIR, ESI-FTICR-MS, and UV–Vis. A diagram showing the developed NOM extraction and purification protocol is shown in Fig. 1 and is described in Section 2.3.1 MQ extracts, 2.3.2 PP extracts. Organic carbon (OC) and metal concentrations were measured in each isolated fraction prior to freeze dryingas well as in whole extracts in order to determine the recovery of OC in each fraction. Solid-free method blanks containing only extracting solutions were tested for the sequential extraction and NOM purification procedures to ensure that there was no contamination present in the samples.

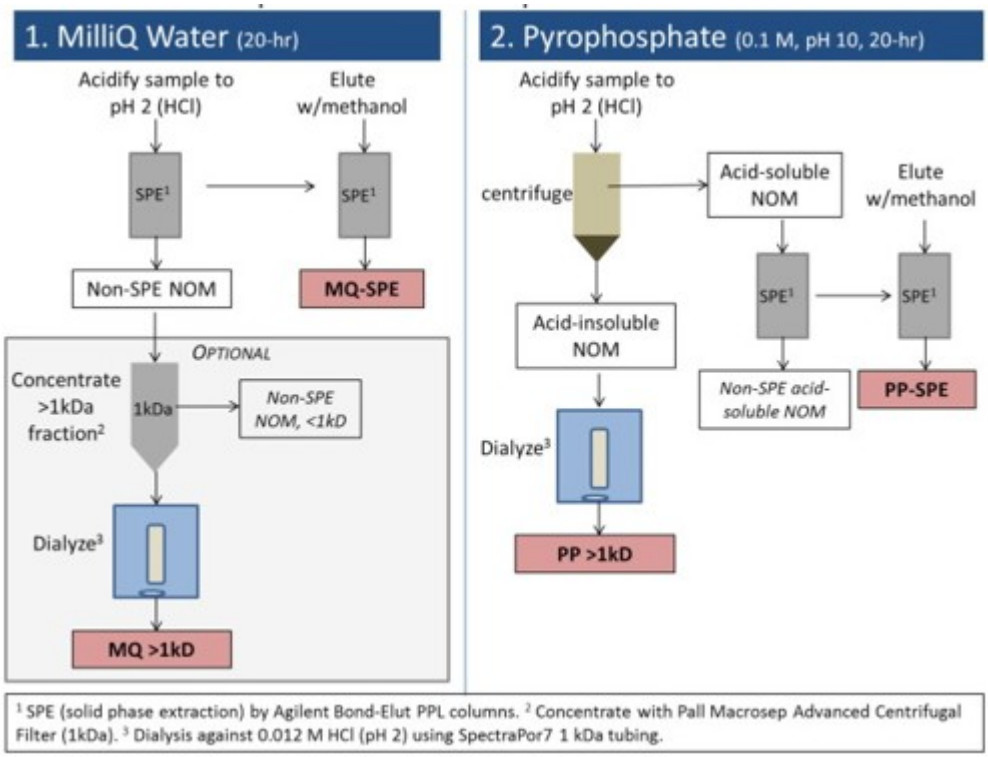

Fig. 1. Schematic diagram showing the NOM sequential extractionand purification protocol applied to sediments.

2.3.1. MQ extracts

MQ extracts were acidified to pH 2 with 1 M HCl, then pumped through a pre-conditioned solid-phase extraction (SPE) column (Agilent Bond-Elut PPL, 100 mg) using a peristaltic pump with Tygon MHLL pump tubing and eluted with 5 mL methanol into a glass vial according to Dittmar et al. (2008). Acidification increases the extraction efficiency for organic acids and phenols (Dittmar et al., 2008). NOM samples dissolved in methanol were then placed in a vacuum desiccator to remove all methanol, redissolved in 5 mL MilliQ water, and freeze-dried. This fraction is referred to as the MQ-SPE fraction.

The fraction of MQ NOM which did not bind to the SPE column was concentrated using pre-rinsed 1 kDa centrifuge filtration units (Pall Macrosep Advanced Centrifugal Filter) by repeatedly adding samples to the 20 mL units and centrifuging at 5000 x *g*. The centrifugal units were filled to a maximum of 15 mL to avoid leakage during centrifugation. The concentrated sample was then transferred to pre-rinsed 1 kDa dialysis tubing (Spectra-Por 7) using approximately 7 mL of 0.012 M HCl (pH 2). The sample was dialyzed against 0.012 M HCl in 1 L glass bottles for approximately 1 week, changing dialysis solution daily. Dialyzed samples were freeze dried. This fraction is referred to as the MQ > 1kD fraction.

2.3.2. PP extracts

PP extracts were acidified to pH 2 with 6 M HCl, resulting in precipitation of a fraction of the NOM. Acidified PP samples were allowed to sit overnight to ensure that NOM precipitation was complete, then centrifuged at 20,000*g* for 30 min to separate the acid-soluble and acid-insoluble NOM. The supernatant (containing acid-soluble NOM) was carefully removed to a clean bottle and then pumped through an SPE column as described in Section 2.3.1. In order to avoid exceeding the sorption capacity of the resin (2 mmol OC/g resin), half the PP sample volume (~80 mL) was passed through the SPE column, eluted with methanol, then the second half of the sample was passed through the SPE column and eluted, and the two eluted fractions were combined and freeze dried as described in Section 2.3.1. This fraction is referred to as the PP-SPE fraction. The precipitated (acid-insoluble) NOM was resuspended in 10 mL 0.012 M HCl, dialyzed against 0.012 M HCl, and freeze dried as described in Section 2.3.1. This fraction is referred to as the PP > 1kD fraction.

2.4. Analytical methods

2.4.1. Sediment TOC

Sediment samples were analyzed for total organic carbon(TOC) by catalytically aided combustion oxidation at 900 °C and a NDIR detector using a Shimadzu TOC-V analyzer equipped with a solids module (SSM) on ball-milled sediments after acid fumigation to remove inorganic carbon. Air-dried sediment was ball-milled using tungsten-carbide balls to a fine powder. Acid fumigation with HCl vapors was performed according to Ramnarine et al. (2011). Total carbon (TC) was measured on non-fumigated ball-milled samples and total inorganic carbon (TIC) determined by difference between TC and TOC. Direct TIC analysis of selected acid-fumigated sediments verified that all inorganic carbon was eliminated by the acid fumigation procedure. TIC analysis was performed by acidification with 20% phosphoric acid and heating to 200 °C in a Shimadzu TOC-V analyzer.

2.4.2. Carbon isotopes

Sediment samples (BH and PP-extracted BH) were shipped to Beta Analytic for ^{14}C radiocarbon dating. The samples were air-dried, crushed, sieved to < 180 μm, and pre-treated with an acid (HCl) wash to remove carbonate minerals prior to analysis of ^{14}C abundance by accelerator mass spectrometry(AMS). Purified NOM extracts (PP-SPE and PP > 1kD fractions) were graphitized in the Houghton Carbon, Water and Soils Lab (USDA-FS Northern Research Station) and radiocarbon measurements were conducted at the KeckCarbon Cycle AMS Facility at UC Irvine. All results have been corrected for isotopic fractionation according to the conventions of Stuiver and Polach (1977), with $\delta^{13}C$ values measured on prepared graphite using the AMS spectrometer. Radiocarbon abundances are given as conventional radiocarbon age, following the conventions of Stuiver and Polach (1977). Conventional age is in radiocarbon years using the Libby half-life of 5568 years. These values are not meant to represent the exact age of the

OC in the dated materials, as the samples contain a mixture of OC compounds with likely variable ages, but are used to compare the average properties across different NOM pools.

2.4.3. Extracted (dissolved) OC and ICP-MS

Extracted organic carbon (OC) concentrations were determined in extract solutions by non-purgeable organic carbon on a Shimadzu TOC-V analyzer. Samples were acidified with HCl and purged with N_2 in order to remove inorganic carbon prior to analysis. Extract solutions were also analyzed for metal concentrations by ICP-MS (Perkin-Elmer Elan DRC II) after acidification and dilution with ultrapure 0.16 M nitric acid and internal standard addition.

2.4.4. FTIR

Freeze-dried NOM samples and ball-milled sediments were analyzed by ATR-FTIR (attenuated total reflection fourier transform infrared spectroscopy) using a Thermo Scientific Nicolet iS50 FTIR equipped with a single-bounce diamond crystal and liquid-N_2 cooled MCT/A detector. Sample spectra were collected from 650 to 4000 cm^{-1}, with 64 scans each. A background spectrum (air) was collected immediately prior to each sample. Atmospheric suppression, ATR-correction, baseline correction, and intensity normalization were performed on background-corrected sample spectra using OMNIC software. Peak assignments are generally taken from Stevenson (1994) and Baes and Bloom (1989). Peak areas were calculated for the CH stretching peaks, which occur as a shoulder (around 2900 cm^{-1}) on the broad O-H stretching peak, using a linear baseline in OMNIC. Peak fitting of the 1500–1800 cm^{-1} region was performed using Igor Pro, whereby the region was fitted with 6 Gaussian peaks, with a linear baseline and a Voigt peak centered around 1450 $cm^{-1}$to account for the contribution from peaks below 1500 cm^{-1}. Duplicate sample extracts were analyzed by FTIR and fitted separately. Fitting results are presented as the average and standard deviation of the duplicates.

2.4.5. UV–Vis absorption

Soluble NOM extracts were analyzed by UV–Vis absorption on a Thermo Scientific Aquamate Plus spectrophotometerover the 200–800 nm wavelength range in a 1-cm quartz cuvette, using a 1 nm step size. Specific UV absorbance($SUVA_{254}$) values were calculated by dividing the absorbance at 254 nm (in m^{-1}) by the OC concentration (in mg/L).

2.4.6. ESI-FTICR-MS

Ultrahigh resolution mass spectrometry of purified sediment extracts was carried out using a 12 Tesla Bruker SolariX Fourier transform ion cyclotron resonance (FT-ICR) mass spectrometer (MS) located at the Environmental Molecular Sciences Laboratory (EMSL) in Richland, WA, USA. Duplicate sample extracts were analyzed by electrospray ionization(ESI)-FTICR-MS in negative ion mode along with method blanks. Samples (dissolved in

methanol) were injected directly into the mass spectrometer and the ion accumulation time was optimized for all samples to account for differences in DOC concentration. A standard Bruker ESI source was used to generate negatively charged molecular ions. Samples were introduced to the ESI source equipped with a fused silica tube (30 μm i.d.) through an Agilent 1200 series pump (Agilent Technologies) at a flow rate of 3.0 μL/min. Experimental conditions were as follows: needle voltage, +4.4 kV; Q1 set to 50 m/z; and the heated resistively coated glass capillary operated at 180 °C. Ninety-six individual scans were averaged for each sample and internally calibrated using an organic matter homologous series separated by 14 Da (–CH_2groups). The mass measurement accuracy was less than 1 ppm for singly charged ions across a broad m/z range (100–900 m/z). The mass resolution was ~350 K at 339 m/z. Data Analysis software (BrukerDaltonik version 4.2) was used to convert raw spectra to a list of m/z values ("features") applying FTMS peak picker with a signal-to-noise ratio (S/N) threshold set to 7 and absolute intensity threshold to the default value of 100.

Chemical formulae were assigned using in-house built software following the Compound Identification Algorithm (CIA), described by Kujawinski and Behn (2006) and modified by Minor et al. (2012). Chemical formulae were assigned based on the criteria listed above and taking into consideration the presence of C, H, O, N, S and P and excluding other elements.

To interpret the resulting large data set, the chemical character of all of the data points for each sample spectrum was evaluated on van Krevelen diagrams on the basis of their molar H:C ratios (*y*-axis) and molar O:C ratios (*x*-axis) (Fenn et al., 1989). Van Krevelen diagrams are used to visualize and compare NOM chemistry between samples and enable approximate grouping of compounds into major biochemical classes (*i.e.*, lipids, proteins, lignin, carbohydrates, and condensed aromatics) (Kim et al., 2003). In this study, biochemical compound classes are reported as relative abundance values based on counts of C, H, and O for the following H:C and O:C ranges: lipids ($0 < O:C \leq 0.3$, $1.5 \leq H:C \leq 2.5$), unsaturated hydrocarbons ($0 \leq O:C \leq 0.125$, $0.8 \leq H:C < 2.5$), proteins ($0.3 < O:C \leq 0.55$, $1.5 \leq H:C \leq 2.3$), amino sugars ($0.55 < O:C \leq 0.7$, $1.5 \leq H:C \leq 2.2$), carbohydrates ($0.7 < O:C \leq 1.5$, $1.5 \leq H:C \leq 2.5$), lignin ($0.125 < O:C \leq 0.65$, $0.8 \leq H:C < 1.5$), tannins($0.65 < O:C \leq 1.1$, $0.8 \leq H:C < 1.5$), and condensed hydrocarbons ($0 \leq 200$ $O:C \leq 0.95$, $0.2 \leq H:C < 0.8$) (Tfaily et al., 2015).

3. Results and discussion

3.1. Evaluation of single extractions

Fig. 2 shows concentrations of OC and selected metals from the single extractions. Files in .csv format containing complete metal concentration data are available for download. As expected, the acidic extractions (HCl and HH) removed higher concentrations of Fe, Al, and Mn than the high pH extractions (PP, NaOH) and water extraction (MQ), presumably due to

dissolution of Fe, Al, and Mn-oxides. Surprisingly, the dithionite extraction produced quite low metal concentrations, with extractable Fe and Al close to the amounts extracted by PP. The extractable OC concentrations follow the opposite trend, with the greatest amounts extracted by PP, followed by NaOH, HCl & HH, and dithionite & MQ. Total sediment organic carbon (TOC) concentrations were 124 ± 2 and 79 ± 1 µmol/g (or 1.49 ± 0.03 and 0.95 ± 0.02 mg/g) for the LRC and BH sediments, respectively. Total sediment inorganic carbon (TIC) concentrations were 549 ± 17 and 334 ± 4 µmol/g (or 6.59 ± 0.20 and 4.01 ± 0.05 mg/g), respectively. The percent of sediment TOC extracted ranged from 0.9–2.6% for the dithionite extractions to 13–15% for the PP extractions, with a greater percentage of OC extracted for the LRC sediment in all cases. One possible reason for the difference in extractability between the two sediments is a difference in the sediment pre-treatment (air-drying for LRC and storing field-moist at 4 °C for BH). Both approaches are common practice in soil science. Air-drying soils greatly reduces the microbial activity, but has been shown to result in an increase in the solubility of organic matter (Bartlett and James, 1980).

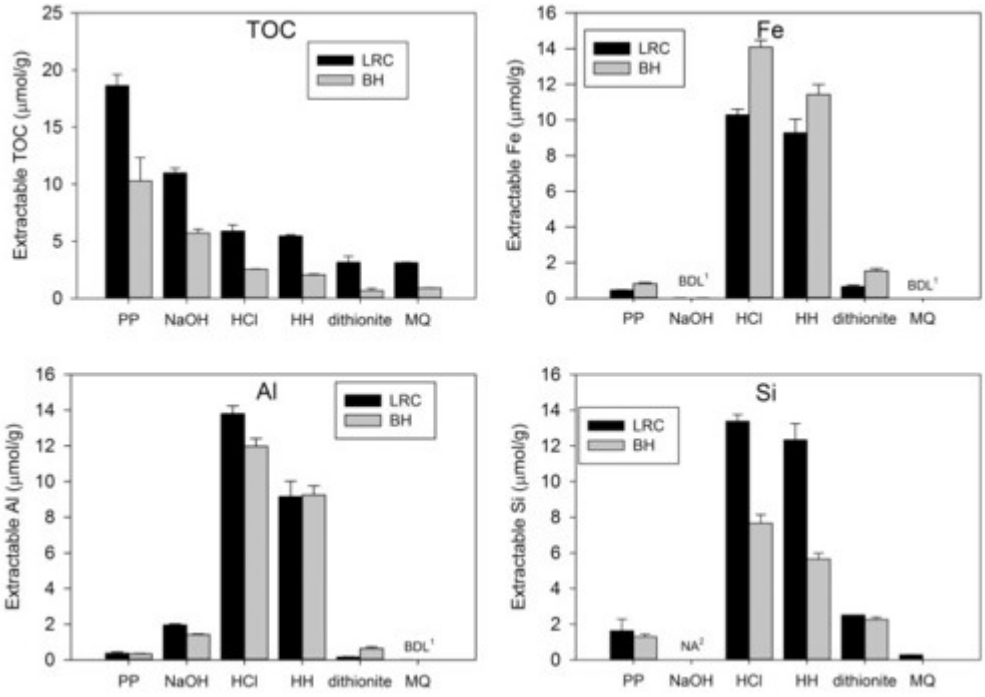

Fig. 2. Extractable organic carbon and metals in various extractions for two sediment samples. Extractions are sodium pyrophosphate (PP), NaOH, HCl, hydroxylamine hydrochloride (HH), inorganic dithionite, and water (MQ). Error bars represent standard deviations of replicate extractions. [1]BDL = below detection limit, [2]NA = data not available, Si concentrations were above the calibration range for NaOH extractions.

Previous citrate-bicarbonate-dithionite extractions of ball-milled LRC sediment showed much higher concentrations of extractable Fe (148 µmol/g) (Fox et al., 2013), indicating that the inefficiency of the inorganic dithionite extraction for Fe, and consequently for OC, may be due to either the lack

of citrate and bicarbonate in the extraction medium and/or to the fact that samples were not ball-milled prior to extraction. Wagai and Mayer (2007) reported recoveries of OC by inorganic dithionite extraction of approximately 2–37% of sediment TOC and extracted Fe concentrations of 27–4600 µmol/g, but they do not state whether samples were ground prior to extraction. Differences between our results and the results of Wagai and Mayer (2007) may be due to differences in grinding (if, in fact they did grind samples), mineralogy, sediment/soil texture, and TOC contents. In particular, the Rifle sediments are calcareous and low in TOC, while none of the samples tested by Wagai and Mayer (2007)appear to be calcareous – most are relatively organic-rich (16–165 mg/g TOC) with acidic-neutral pH values (pH 4.0–6.2) and there appears to be a negative correlation between dithionite-extractable OC and soil pH in their data (Wagai and Mayer, 2007). Lopez-Sangil and Rovira (2013) found that pyrophosphate extracted the greatest amount of OC from calcareous soils in a sequential extraction procedure, whereas sodium tetraborate (pH 9.7), which does not complex metals, extracted the most OC from granitic soils. They attributed this difference to the stabilizing effect of Ca, which can cause flocculation and precipitation of NOM. Similar effects may be responsible for the low OC extraction during dithionite extractions. Other possible explanations for lower extractability in calcareous materials include sorption of NOM to carbonate minerals, and coating of NOM and Fe oxide minerals by carbonates, making Fe-oxides less susceptible to attack by dithionite. Inclusion of citrate in the extraction media would be expected to promote the release of adsorbed and flocculated OC through ligand exchange (*i.e.*, competition for adsorption sites) and metal complexation. The inclusion of a dilute HCl rinse following the dithionite extraction is designed to redissolve any FeS produced due to the lack of citrate and bicarbonate in the extraction media (Wagai and Mayer, 2007), and should dissolve most carbonate minerals in the sediments. However, only acid-soluble NOM will be released by HCl.

A comparison of NaOH and PP extracts may provide insight into the role of mineral-association and metal-complexation of NOM in our sediments. Although both extractions are alkaline (pH 13.7 and 10 for NaOH and PP, respectively), PP chelatesmetals, thereby releasing NOM stabilized by metals through ligand exchange, metal complexation and aggregation (Pansu and Gautheyrou, 2006). PP extractions released 13–15% of the sediment TOC compared to 7–9% released by NaOH, indicating that high pH alone was not responsible for the release of carbon, but rather a large fraction of the PP-extracted carbon was stabilized by metals. Higher concentrations of Fe, Mn, Ca, and Mg in the PP extracts (Fig. 1 and SI) provide further evidence that complexation of NOM by metals may play an important role in sequestering NOM in these sediments. Al concentrations are higher in the NaOH extracts, most likely due to partial dissolution of clay minerals. These results contrast those of Wagai et al. (2013) where similar amounts of N were extracted

using PP and sodium carbonate (pH 10), with the exception of some volcanic soilsfor which higher concentrations were reported for PP extractions. These differences may reflect a difference in the dominant chemical forms of NOM in high OC and low OC soils and sediments, with a greater fraction of OC present in the adsorbed fraction in high OC soils. Mineralogical differences may also play a role. For example, as discussed above, pyrophosphate has been shown to extract more OC than sodium tetraborate (pH 9.7) in carbonate-rich soils, likely due to the complexation of NOM with Ca (Lopez-Sangil and Rovira, 2013). Pyrophosphate has also been shown to be more efficient than NaOH at extraction of NOM from smectiteclays, while the reverse is true for kaolinite (Wattel-Koekkoek et al., 2001). Based on an analysis of the ratio of TOC to pyrophosphate-extractable Fe and Al in grassland soilscollected from a chronsequence, Masiello et al. (2004)suggested that metal chelation may be the single most important parameter controlling carbon storage in the deeper horizons of undeveloped (young) soils and in all horizons of developed soils in their study.

3.2. Sequential extractions

Based on the results of the single extractions, a sequential extraction procedure was developed using water and pyrophosphate, and the extracted NOM was purified to allow for chemical characterization. This combination of extractants was chosen for three reasons: (1) to allow for comparison with results from a similar sequential extraction procedure developed and employed in relatively high-C surface soils, (2) PP was most effective at releasing NOM compared to HCl, HH, and dithionate extractions, and (3) the two functional pools targeted by water and pyrophosphate are hypothesized to be particularly important in the cycling of organic matter, representing a highly labile and a much less labile pool, respectively. The sequential extraction and purification procedure produced four different isolated and purified NOM fractions: MQ-SPE, MQ > 1kD, PP-SPE, and PP > 1kD. The two SPE fractions were light to medium brown in color with a cotton-like fibrous texture, while the PP > 1kD fraction was nearly black with a granular texture (pictures in SI). A summary of OC recovery and chemical properties of the extracts and isolated NOM fractions are shown in Table 2.

Table 2. Organic carbon (OC) recoveries, $SUVA_{254}$ values, pH values, and metal:OC ratios for various fractions of water (MQ) and sodium pyrophosphate (PP) sequential extractions of LRC sediment. Metal:OC ratios are expressed as a mol% (100 × mol metal/mol OC).

Fraction	OC (µmol/g)	$SUVA_{254}$ (L/mg-m)	pH	Mg:OC (mol%)	Al:OC	Si:OC	Fe:OC
whole MQ	3.1 ± 0.03	2.1 ± 0.2	8.6	42.6	0.14	9.00	BDL[a]
MQ-SPE	0.80 ± 0.03	3.5 ± 0.1	3.8	0.15	0.09	0.32	0.02
MQ > 1 kD	0.08 ± 0.01	–[b]	2.0	BDL	0.94	0.94	0.22
whole PP	17.4 ± 0.5	–	10.3	37.6	1.35	6.80	2.45
PP-SPE	3.33 ± 0.99	5.4 ± 0.1	3.1	BDL	0.04	0.93	0.03
PP > 1 kD	8.03 ± 0.96	–	2.0	0.02	0.15	0.24	0.25

a BDL = below detection limit.

b not measured.

3.2.1. Recoveries and metal contents of isolated NOM

Many literature studies which employ extraction and purification protocols for the isolation of soil-associated NOM do not report recoveries of carbon in their extracted fractions or the loss of carbon during purification. This makes it difficult to determine (1) the size of the different extracted pools of NOM and (2) how representative the various purified pools are in relation to the total extracted NOM. We have quantified the OC in each fraction of our protocol in order to provide a basis for making these assessments and the results are shown in Table 2 and Fig. S8 (in SI). A total of 20.5 ± 0.5 µmol/g OC was recovered by sequential extraction of LRC sediment with MQ and PP, corresponding to 2.5 and 13.4% of total sediment OC, respectively. Within the MQ-extractable fraction, 25.7% was recovered in the MQ-SPE fraction and only 2.5% in the MQ > 1kD fraction. By contrast, 46.2% of the PP-extractable OC was recovered in the PP > 1kD fraction (acid insoluble), with 47.8% in the acid soluble fraction. The PP-SPE fraction accounted for 40.0% of the acid-soluble PP-extractable OC (or 19.1% of the total PP-extractable OC). A similar distribution of PP-extracted OC between acid soluble and insoluble fractions is reported for forest soils (Kaiser et al., 2016). The

difference in the OC recovered by dialysis between the MQ and PP fractions suggests that there is a difference in the average apparent molecular weight (MW) in these fractions. The apparent MW (*i.e.*, as determined by dialysis or size-exclusion chromatography) of NOM is known to be influenced by factors other than molecular size such as charge and polarity, which promote aggregation and the formation of supramolecular associations (Piccolo, 2001, Sutton and Sposito, 2005). We found that solution pH strongly affected the recovery of NOM in the PP > 1kD fraction; acidification of PP solution to pH 2 and dialysis with 0.012 M HCl (pH 2) instead of MilliQ water increased recovery by dialysis from 25 to 46.2%, presumably due to greater aggregation at pH 2. The increase in recovery appeared to be primarily due to an increase in carboxylic-rich and possibly phenolic-rich compounds, which should be protonated at pH 2 (see SI for details). This observation is consistent with the important role of hydrogen bonding in NOM aggregation at low pH (Piccolo, 2001). Because protonation is reversible, the fundamental molecular properties of the NOM should not be affected by the acidification step. Due to the low amount of OC recovered in the MQ > 1kD fraction, this step is listed as optional in the separation scheme (Fig. 2) and no further characterization of this fraction was performed.

The NOM purification procedures (SPE and dialysis) significantly decreased metal and major cation concentrations in the extracts (Table 2 and SI). For example, Fe:OC molar ratios decreased from 2.5 mol% in the PP extract (whole PP) to 0.03 and 0.25 mol% in the PP-SPE and PP > 1kD fractions, respectively. The decrease in inorganic components is a necessary step for characterization of NOM by FTIR, ESI-FTICR-MS, and UV absorbance, particularly for the PP extracts due to interference of the inorganic components in the analysis (Reemtsma, 2009, Poulin et al., 2014). However, it is important to note that some metals persisted in the NOM, indicating that these metals are strongly bound to or incorporated into the organic structure. Iron and aluminum concentrations were approximately 10 times higher in the > 1kD fractions than the SPE fractions for both MQ and PP and may be acting as cation bridges among organic constituents in this fraction. This may result in stronger macromolecular associations, which increase the apparent molecular weight of this fraction and lead to retention within the 1 kDa membrane.

3.3. Characterization of isolated NOM

3.3.1. UV–Vis absorbance

UV absorbance was measured on extracted NOM fractions and the $SUVA_{254}$ (specific UV absorbance at 254 nm) was determined (Table 2). $SUVA_{254}$ values were higher for the PP-SPE fraction (5.4 L/mg-m) than the MQ-SPE fraction (3.5 L/mg-m). $SUVA_{254}$ values are positively correlated with aromaticity (Weishaar et al., 2003), indicating that the PP-SPE fraction is more aromatic in nature than the MQ-SPE fraction. The $SUVA_{254}$ of the whole MQ fraction was slightly lower than the MQ-SPE fraction, suggesting that the

SPE fraction may be slightly more aromatic than the whole water-extractable pool. Full UV absorbance spectra are shown in the SI. UV absorbance was not measured on whole PP or PP > 1kD fractions due to interferences from Fe (whole PP) and insoluble NOM (PP > 1kD).

3.3.2. FTIR

FTIR spectra were collected on the MQ-SPE, PP-SPE, and PP > 1kD fractions isolated from LRC sediment (Fig. 3 and SI). Insufficient material was recovered for the MQ > 1kD fraction for FTIR analysis. The largest differences observed between these fractions are in the OH stretching region (~3380 cm^{-1}), CH stretching region (~2900 cm^{-1}) and the CO and CC stretching region (1500–1800 cm^{-1}). The MQ-SPE fraction had the largest CH peaks. The importance of COC type bonds at 1030 and 1080 cm^{-1}, sometimes indicative of polysaccharides, appeared to be fairly low in all three samples, although there were some small differences between the fractions.

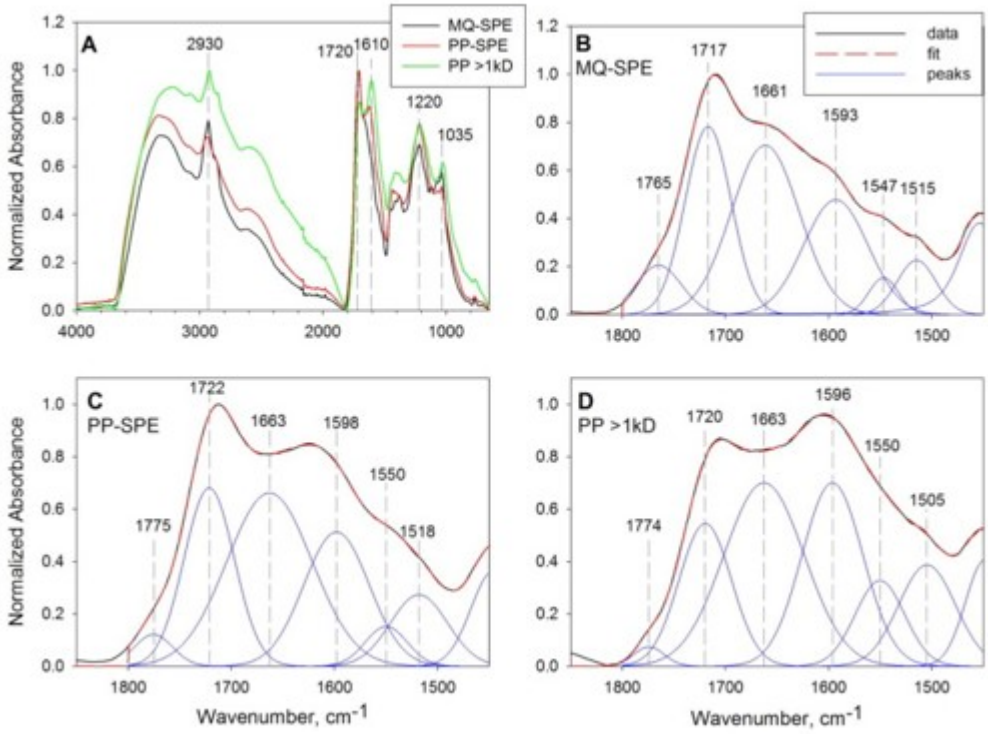

Fig. 3. Normalized ATR-FTIR spectra for isolated NOM fractions from LRC sediment. (A) Comparison of extracts over entire spectral range, and close up of 1500–1800 cm^{-1} with peak fits for (B) MQ-SPE, (C) PP-SPE, and (D) PP > 1kD fractions.

In order to better resolve the CO and CC peaks, peak fitting was performed on this region and results are shown in Fig. 3, Fig. 4. Peak fitting revealed that the MQ-SPE fraction had the highest fraction of carboxylic acid groups (COOH peak at 1720 cm^{-1}) and the PP > 1kD fraction had the lowest. The peak at 1775 cm^{-1} is not typically assigned, but may represent esters or anhydrides, and was also higher in the MQ-SPE fraction.

The peak at 1660 cm^{-1} was the largest peak in all three samples and is typically assigned to the CO stretch of amides, but may also represent CO conjugated with aromatic rings (Derkacheva and Sukhov, 2008). A comparison of the peaks at 1720 and 1660 cm^{-1} indicates that the MQ-SPE fraction had a larger fraction of CO groups fully oxidized to COOH compared to the PP-SPE and PP > 1kD fractions. While it is difficult to assign the peaks at 1600 and 1550 cm^{-1} definitively due to the presence of a carboxylate (COO^-) peak in that region, the carboxylate peak tends to be centered closer to 1585 cm^{-1} with a corresponding peak at 1375 cm^{-1} in NOM (Hay and Myneni, 2007). The absence of a large peak at 1375 cm^{-1} and the presence of peaks at 1220 and 2600 cm^{-1} in our spectra, which are indicative of COOH (Baes and Bloom, 1989), suggests that the majority of the carboxyl groups were protonated in these samples and there was a relatively minor contribution from COO^- groups in the peaks at 1600 and 1550 cm^{-1}. Furthermore, both of these peaks were largest in the fraction with the lowest pH (PP > 1kD, pH 2.05) and smallest in the highest pH fraction (MQ-SPE, pH 3.77). Therefore, we can assume that the peak at 1600 cm^{-1} was primarily due to CC stretching. The peak near 1515 $cm^{-1}$was likely also representative of aromatic CC stretching (Baes and Bloom, 1989, Haberhauer et al., 1998, Derkacheva and Sukhov, 2008), however there was some ambiguity between the peaks at 1515 and 1550 cm^{-1} in our fitting, particularly for the PP > 1kD fraction resulting in shifting peak positions (Fig. 4 and SI). The larger CC stretching peaks in the PP > 1kD sample may be due to a larger fraction of phenolic compounds, as the OH stretching region (2500–3600 cm^{-1}) was also larger in this sample (Fig. 3A).

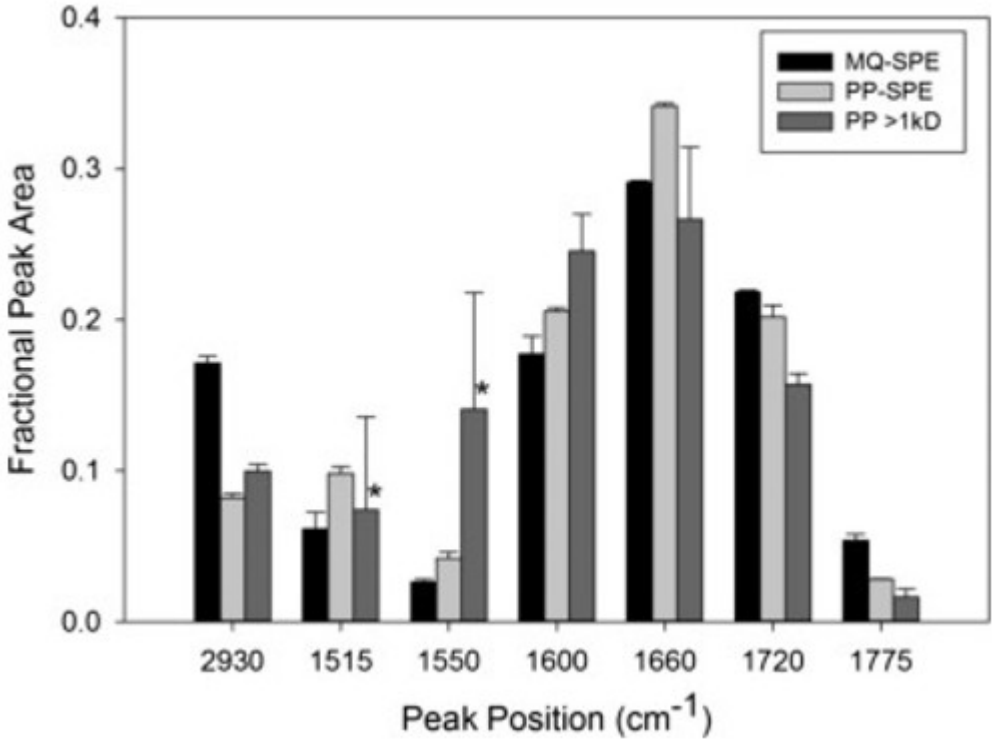

Fig. 4. Relative peak areas for peaks identified in the 1500–1800 cm^{-1} range from peak fitting. Peak areas for CH stretching peaks at 2850–2950 cm^{-1} are also shown. * Note that the peak positions for the PP > 1kD fraction shifted to ~1500 and 1540 cm^{-1}.

A comparison of the chemical characteristics of the extracted NOM in this study with that extracted from surface soils using a similar extraction scheme reveal both similarities and differences. The largest contrast is that the organic matter extracted by both water and pyrophosphate from surface soils showed a dominant peak at ~1081 cm^{-1} indicative of a large fraction of COC and/or SiO functionality, and it was this peak that changed the most between the water and pyrophosphate extractable material (Ellerbrock and Kaiser, 2005, Kaiser and Ellerbrock, 2005, Kaiser et al., 2007). By contrast, the peak at 1081 cm^{-1} was comparatively minor and relatively invariant between extracts in our study. This result indicates an effective separation of the organic phase from the mineral fraction in this study, removing the need to “ash correct” the reported spectra. It may also indicate a smaller fraction of polysaccharide type molecules in the sediment organic matter as compared to the surface soils, as the difference persists even when the surface soil spectra are ash corrected (Kaiser et al., 2011, Kaiser et al., 2012). Similarly to our results, the water extractable fraction showed a larger signal in the ~2900 cm^{-1} CH region compared to the pyrophosphate-extractable OC (Ellerbrock and Kaiser, 2005, Kaiser and Ellerbrock, 2005, Kaiser et al., 2007). However, in contrast to our study, the CO/CC peaks in the 1500–1800 cm^{-1} region (referred to as Band B in their study) were larger in the PP-extract than the water extract (Ellerbrock and Kaiser, 2005, Kaiser and Ellerbrock, 2005, Kaiser et al., 2007). Differences in CH and CO/CC peaks between the acid soluble and acid insoluble PP-extracts are very similar to those observed in our study (Ellerbrock and Kaiser, 2005). In addition to possible differences in NOM from surface soils and subsurface sediments, some methodological differences may help explain differences between results of our study and those of Kaiser and colleagues (Ellerbrock and Kaiser, 2005, Kaiser and Ellerbrock, 2005, Kaiser et al., 2007). In those studies, dialysis against water is used for purification of both water soluble and PP-extractable NOM, whereas our study used both SPE and dialysis against dilute HCl (pH 2). Both SPE and dialysis against acid are expected to increase recovery of carboxyl and phenolic compounds (Dittmar et al., 2008 and this study, results shown in SI). Recent work has shown that the residual fraction of organic matter in surface soil after extraction with pyrophosphate tends to be lower in carbonyl groups relative to the extracted material (Kaiser et al., 2016). Wattel-Koekkoek et al. (2001)showed that residual OC associated with clay minerals after NaOH and pyrophosphate extraction was largely aliphatic.

3.3.3. ESI-FTICR-MS

All three isolated NOM fractions were analyzed by ESI-FTICR-MS. A large number of compounds with different characteristics and spanning O/C range between 0.1–0.9 and H/C range between 0.5–2 were detected in the MQ-SPE

and PP-SPE fractions (approximately 4600 and 2400 after blank correction, respectively). The PP-SPE fraction had compounds with a higher average mass (469) compared to the MQ-SPE fraction (430). However, despite the high concentrations of OC in the PP acid insoluble > 1kD fraction, very few compounds were detected in this fraction even when the m/z detection range was increased to 30,000 (data not shown). This may be due to low ionizability of the presumably larger molecules in this fraction (Reemtsma, 2009). In general, molecules can only efficiently ionize during ESI is when they are able to stabilize a negative charge and thus ESI acidic functional groups such as carboxylic acids are easily deprotonated and therefore are preferentially ionized relative to alcohols, alkyl groups, and /or carbohydratemolecules. Duplicate samples analyzed for each NOM fraction revealed high reproducibility between replicates, with 83% and 82% of the comopounds in common for the MQ-SPE and PP-SPE fractions, respectively. Mass spectra and van Krevelen diagrams are shown for each replicate in the SI.

A comparison of the MQ-SPE and PP-SPE samples is shown in van Krevelen diagrams in Fig. 5. The number of compounds common to both MQ-SPE and PP-SPE fractions accounted for 33–35% of the MQ-SPE compounds and 64–67% of the PP-SPE compounds. This suggests that the MQ-SPE fraction was more diverse than the PP-SPE fraction, however, there were still a reasonably large number of compounds (>33%) unique to the PP-SPE fraction. The MQ-SPE fraction had a higher abundance of compounds in the low O/C and high H/C region (0–0.4 O/C, 0.8–2.0 H/C), suggesting that MQ was selective for extracting more highly saturated compounds with low degrees of oxidation, such as lipids, proteins, and lignins (compound class assignments are shown in the SI) compared to PP. This is consistent with our observation of larger CH stretching peaks in the FTIR spectra and lower $SUVA_{254}$ values of the MQ-SPE fraction compared to the PP-SPE fraction. The observation of a greater abundance of both highly saturated aliphatic compounds and carboxylic-rich compounds (from FTIR data) in the MQ-SPE fraction provides further evidence of the diverse nature of this fraction. The PP fraction on the other hand had a higher abundance of compounds with high O/C ratios and low H/C ratios suggesting that PP is selective for extracting condensed aromatic compounds and tannin-like compounds, consistent with higher $SUVA_{254}$ values in the PP fraction and larger CC and phenolic peaks in the FTIR spectra.

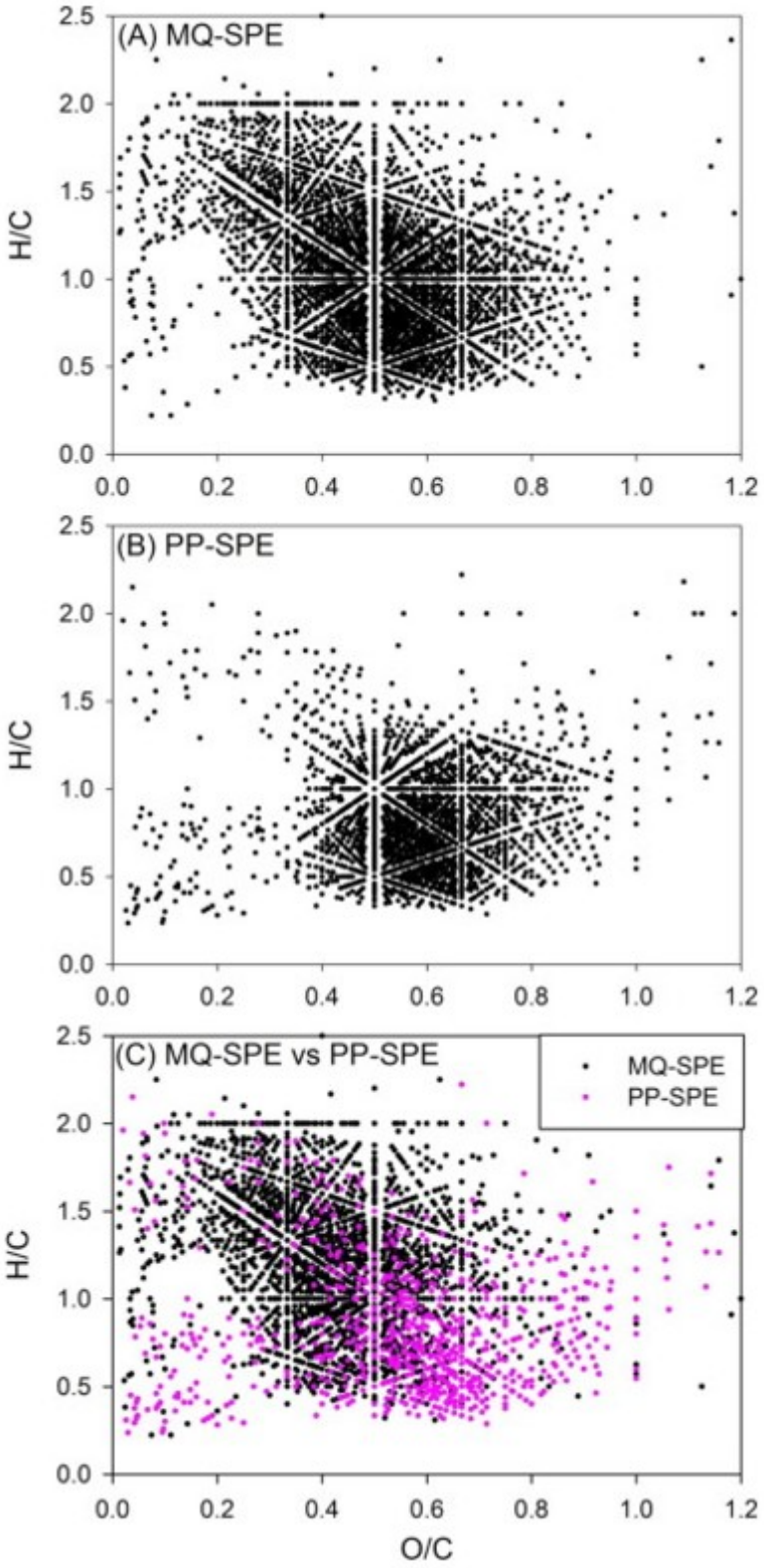

Fig. 5. Example ESI-FTICR-MS van Krevelen diagrams showing all peaks for (A) MQ-SPE and (B) PP-SPE fractions of NOM isolated from LRC sediment, and (C) comparison of unique peaks for MQ-SPE (black)

and PP-SPE (pink). (For interpretation of the references to colour in this figure legend, the reader is referred to the web version of this article.)

3.3.4. ^{14}C results

Radiocarbon abundance was measured on purified extracts (PP-SPE and PP > 1kD), residual (non-extractable) sediment NOM, and whole (non-extracted) sediment for the BH sediment sample in order to provide further insight into the nature of these different pools of NOM. Within the PP-extractable fraction, ^{14}C measurements yielded standard radiocarbon ages of 1020 and 3095 years BP for the PP-SPE and PP > 1kD fractions of the BH sediment. Others have observed that water-extractable carbon is younger than PP-extractable carbon (*i.e.*, has a higher radiocarbon abundance) (Ellerbrock and Kaiser, 2005, Kaiser and Ellerbrock, 2005), providing evidence for the stability of the Fe-associated pool of NOM. The residual, non-extractable NOM was much older (*i.e.*, lower radiocarbon abundance), with a standard radiocarbon age of 9360 years BP, while the whole (non-extracted) sediment yielded a bulk radiocarbon age of 8160 years BP. Kaiser et al. (2016) observed a similar trend of residual OC being older than pyrophosphate-extractable OC in some forest soils, however the mean residence times were all less than 100 years for all of their soils. The low radiocarbon abundance of the original sediment OC in our study indicates that the carbon was likely closely associated with the mineral phase prior to the deposition of sediments in this alluvial aquifer. By contrast, detrital organic matter collected from sediment cores in this aquifer ranged from 110 to 180 ± 30 years BP (Janot et al., 2016), and is expected to be representative of the depositional age of sediments. It is possible that some of the sediment-associated OC pool is ‘isotopically dead’ carbon (*e.g.*, derived from ancient sedimentary kerogen and > 50,000 years old), thereby biasing the average age of the entire pool. Based on the observed ^{14}C ages, it is likely that most of the kerogen OC resides in the residual fraction.

4. Conclusions and implications

Most of the literature describing chemical characterization of soil NOM has been performed on samples with relatively high organic carbon concentrations (*i.e.*, 10–200 mg/g), due in large part to the analytical challenges associated with characterization of low-carbon soils/sediments. We evaluated a series of extractions for OC extraction efficiency and developed an extraction and purification protocol for samples with TOC concentrations 10–100 times lower than the typical surface soils. Direct measurements of soil NOM (*e.g.*, through FTIR and NMR) are practically impossible to do on such low-carbon samples. We collected FTIR data on whole sediments, however, due to the extremely low concentrations of OC in comparison to the clay and silica mineral content, the data were not useful (see SI for details) even when ash corrected. By contrast, the data quality of our extracted and purified NOM was very high and unaffected by mineral impurities. Chemical characterization of these extracted pools of NOM through UV absorbance, FTIR, and FTICR-MS demonstrated a trend from

more aliphatic and carboxyl-rich to more aromatic in the order MQ-SPE, PP-SPE, and PP > 1kD. NOM extracted with this protocol showed similar characteristics to NOM extracted in high-C surface soils (Ellerbrock and Kaiser, 2005, Kaiser and Ellerbrock, 2005, Kaiser et al., 2007), with the most notable difference observed in the relative proportion of polysaccharide-like compounds (COC peaks). ^{14}C measurements followed a similar trend, with standard radiocarbon ages of 1020, 3095, and 9360 years BP for the PP-SPE, PP > 1kD, and residual (non-extractable) fractions, respectively, indicating the extractions targeted functionally different pools of carbon. The low number of compounds detected for the PP > 1kD fraction by FTICR-MS in spite of high OC recovery in this fraction emphasizes the need for multiple lines of investigation, as each analytical techniquehas different types of biases.

The chemical nature of NOM impacts its reactivity towards metals, minerals, and enzymes (Baldock and Skjemstad, 2000 and references therein; Kaiser and Guggenberger, 2000) and is one key piece of information needed to understand the preservation or degradation of soil NOM. Despite low OC concentrations in the subsurface, approximately half of the soil carbon may be stored in the deeper subsurface (> 1 m) (Trumbore et al., 1995). It is largely unknown whether subsurface carbon behaves similarly to carbon in high-C surface soils with respect to climate change(Conen et al., 2006, Smith et al., 2008, Conant et al., 2011, Rumpel and Kögel-Knabner, 2011). A combination of physical protection and molecular structure may play a role in the resistance of soil OC to degradation (Kleber, 2010, Kleber et al., 2011, Schmidt et al., 2011). The extraction approach developed in this study can be a useful tool to probe the variation in NOM chemical composition and mineral association across different biogeochemical regimes and assess the potential reactivity and stability of various NOM pools. In fact, sequential extraction can provide information not only on the chemical properties of soil NOM, but on the relative stabilities of various NOM pools and the mechanisms controlling this stability as demonstrated by the different ^{14}C contents. While the MQ-SPE fraction represents a highly labile and mobile pool of NOM, the PP-extractable fractions are stabilized in the solid phase through metal complexationand therefore are more resistant to mobilization and degradation. Within the PP-extractable NOM, the PP > 1kD fraction is the oldest and presumably most resistant to degradation, possibly due to greater metal complexation, higher apparent molecular weight, and greater degree of aromaticity. The residual (non-extractable) fraction of NOM is even older, representing a pool of NOM most likely derived from shale kerogen that is most resistant to degradation either due to stabilization by the mineral phase or chemical recalcitrance.

Acknowledgements

The authors thank Dr. John Bargar (SSRL) for facilitating ^{14}C measurements of sediments and Dr. Kenneth H. Williams (LBL) for assistance with sediment collection. The authors thank two anonymous reviewers and Dr. Joseph

Curiale for constructive comments on this manuscript. Funding for this study was provided by the U.S. Department of Energy, BERContract DE-AC020SCH11231 to the LBNL Sustainable Systems Scientific Focus Area. FTICR-MS analysis was performed using EMSL, a DOE Office of Science User Facility sponsored by the Office of Biological and Environmental Research. Radiocarbon analysis was supported in part by the Radiocarbon Collaborative, which is jointly sponsored by the USDA Forest Service Northern Research Station, the KCCAMS Facility at UC Irvine, and Michigan Technological University.

References

Baes and Bloom, 1989

A.U. Baes, P.R. Bloom**Diffuse Reflectance and Transmission Fourier Transform Infrared (DRIFT) spectroscopy of humic and fulvic acids**

Soil Science Society of America Journal, 53 (1989), pp. 695-700

Baldock and Skjemstad, 2000

J.A. Baldock, J.O. Skjemstad**Role of the soil matrix and minerals in protecting natural organic materials against biological attack**

Organic Geochemistry, 31 (2000), pp. 697-710

Bartlett and James, 1980

R. Bartlett, B. James**Studying dried, stored soil samples – some pitfalls**

Soil Sci. Soc. Am. J., 44 (1980), pp. 721-724

Campbell et al., 2012

K.M. Campbell, R.K. Kukkadapu, N.P. Qafoku, A.D.Peacock, E. Lesher, K.H. Wil liams, J.R. Bargar, M.J. Wilkins, L.Figueroa, J. Ranville, J.A. Davis, P.E. Long**Ge ochemical, mineralogical and microbiological characteristics of sediment from a naturally reduced zone in a uranium-contaminated aquifer**

Applied Geochemistry, 27 (2012), pp. 1499-1511

Chao and Zhou, 1983

T. Chao, L. Zhou**Extraction techniques for dissolution of amorphous iron oxides from soils and sediments**

Soil Science Society of America Journal, 47 (1983), pp. 225-232

Conant et al., 2011

R.T. Conant, M.G. Ryan, G.I. Ågren, H.E. Birge, E.A.Davidson, P.E. Eliasson, S. E. Evans, S.D. Frey, C.P. Giardina, F.M.Hopkins, R. Hyvönen, M.U.F. Kirschbau m, J.M. Lavallee, J. Leifeld, W.J. Parton, J. Megan
Steinweg, M.D. Wallenstein, J.Å. Martin
Wetterstedt, M.A. Bradford**Temperature and soil organic matter**

decomposition rates – synthesis of current knowledge and a way forward

Global Change Biology, 17 (2011), pp. 3392-3404

Conen et al., 2006

F. Conen, J. Leifeld, B. Seth, C. Alewell**Warming mineralises young and old soil carbon equally**

Biogeosciences, 3 (2006), pp. 515-519

Derkacheva and Sukhov, 2008

O. Derkacheva, D. Sukhov**Investigation of lignins by FTIR spectroscopy**

Macromolecular Symposia, 265 (2008), pp. 61-68

de la Rosa et al., 2011

J.M. de la Rosa, J.A. González-Pérez, F.J.González-Vila, H. Knicker, M.F. Araújo**Molecular composition of sedimentary humic acids from South West Iberian Peninsula: a multi-proxy approach**

Organic Geochemistry, 42 (2011), pp. 791-802

DiDonato et al., 2016

N. DiDonato, H. Chen, D. Waggoner, P.G. Hatcher**Potential origin and formation for molecular components of humic acids in soils**

Geochimica et Cosmochimica Acta, 178 (2016), pp. 210-222

Dittmar et al., 2008

T. Dittmar, B. Koch, N. Hertkorn, G. Kattner**A simple and efficient method for the solid-phase extraction of dissolved organic matter (SPE-DOM) from seawater**

Limnology and Oceanography: Methods, 6 (2008), pp. 230-235

DOE, 1999

DOE, 1999. Final Site Observational Work Plan for the UMTRA project Old Rifle site, Grand Junction, CO, Document U0042501.

Ellerbrock and Kaiser, 2005

R.H. Ellerbrock, M. Kaiser**Stability and composition of different soluble soil organic matter fractions–evidence from δ^{13}C and FTIR signatures**

Geoderma, 128 (2005), pp. 28-37

Fenn et al., 1989

J. Fenn, M. Mann, C. Meng, S. Wong, C. Whitehouse**Electrospray ionization for mass spectrometry of large biomolecules**

Science, 246 (1989), pp. 64-71

Fischlin et al., 2007

A. Fischlin, G.F. Midgley, J.T. Price, R. Leemans, B.Gopal, C. Turley, M.D.A. Rounsevell, O.P. Dube, J. Tarazona, A.A.Velichko**Ecosystems, their properties, goods, and services**

M.L. Parry, O.F. Canziani, J.P. Palutikof, P.J. van der Linden, C.E.Hanson (Eds.), Climate Change 2007: Impacts, Adaptation, and Vulnerability. Contribution of Working Group II to the Fourth Assessment Report of the Intergovernmental Panel on Climate Change, Cambridge University Press, Cambridge (2007), pp. 211-272

Fox et al., 2012

P.M. Fox, J.A. Davis, M.B. Hay, M.E. Conrad, K.M.Campbell, K.H. Williams, P.E. Long**Rate-limited U(VI) desorption during a small-scale tracer test in a heterogeneous uranium-contaminated aquifer**

Water Resources Research, 48 (2012), p. W05512

Fox et al., 2013

P.M. Fox, J.A. Davis, R. Kukkadapu, D.M. Singer, J.Bargar, K.H. Williams**Abiotic U(VI) reduction by sorbed Fe(II) on natural sediments**

Geochimica et Cosmochimica Acta, 117 (2013), pp. 266-282

González-Pérez et al., 2014

J.A. González-Pérez, G. Almendros, J.M. de la Rosa, F.J. González-Vila**Appraisal of polycyclic aromatic hydrocarbons (PAHs) in environmental matrices by analytical pyrolysis (Py–GC/MS)**

Journal of Analytical and Applied Pyrolysis, 109 (2014), pp. 1-8

Haberhauer et al., 1998

G. Haberhauer, B. Rafferty, F. Strebl, M.H.Gerzabek**Comparison of the composition of forest soil litter derived from three different sites at various decompositional stages using FTIR spectroscopy**

Geoderma, 83 (1998), pp. 331-342

Hay and Myneni, 2007

M.B. Hay, S.C.B. Myneni**Structural environments of carboxyl groups in natural organic molecules from terrestrial systems. Part 1: Infrared spectroscopy**

Geochimica et Cosmochimica Acta, 71 (2007), pp. 3518-3532

Heckman et al., 2011

K. Heckman, A. Vazquez-Ortega, X. Gao, J.Chorover, C. Rasmussen**Changes in water extractable organic matter during incubation of forest floor material in the presence of quartz, goethite and gibbsite surfaces**

Geochimica et Cosmochimica Acta, 75 (2011), pp. 4295-4309

Hyun et al., 2009

S.P. Hyun, P.M. Fox, J.A. Davis, K.M. Campbell, K.F.Hayes, P.E. Long**Surface complexation modeling of U(VI) adsorption by aquifer sediments from a former mill tailings site at Rifle, Colorado**

Environmental Science & Technology, 43 (2009), pp. 9368-9373

Ikeya et al., 2012

K. Ikeya, R.L. Sleighter, P.G. Hatcher, A. Watanabe**Compositional features of Japanese humic substances society standard soil humic and fulvic acids by Fourier transform ion cyclotron resonance mass spectrometry and x-ray diffraction profile analysis**

Humic Substances Research, 9 (2012), pp. 25-33

Ikeya et al., 2015

K. Ikeya, R.L. Sleighter, P.G. Hatcher, A. Watanabe**Characterization of the chemical composition of soil humic acids using Fourier transform ion cyclotron resonance mass spectrometry**

Geochimica et Cosmochimica Acta, 153 (2015), pp. 169-182

Janot et al., 2016

N. Janot, J.S. Lezama
Pacheco, D.Q. Pham, T.M.O'Brien, D. Hausladen, V. Noël, F. Lallier, K. Maher, S. Fendorf, K.H. Williams, P.E. Long, J.R. Bargar**Physico-Chemical Heterogeneity of Organic-Rich Sediments in the Rifle Aquifer, CO: Impact on Uranium Biogeochemistry**

Environmental Science & Technology, 50 (2016), pp. 46-53

Kaiser and Guggenberger, 2000

K. Kaiser, G. Guggenberger**The role of DOM sorption to mineral surfaces in the preservation of organic matter in soils**

Organic Geochemistry, 31 (2000), pp. 711-725

Kaiser and Ellerbrock, 2005

M. Kaiser, R.H. Ellerbrock**Functional characterization of soil organic matter fractions different in solubility originating from a long-term field experiment**

Geoderma, 127 (2005), pp. 196-206

Kaiser et al., 2007

M. Kaiser, R.H. Ellerbrock, H.H. Gerke**Long-term effects of crop rotation and fertilization on soil organic matter composition**

European Journal of Soil Science, 58 (2007), pp. 1460-1470

Kaiser et al., 2012

M. Kaiser, R.H. Ellerbrock, M. Wulf, S. Dultz, C. Hierath, M. Sommer**The influence of mineral characteristics on organic matter content, composition, and stability of topsoils under long-term arable and forest land use**

Journal of Geophysical Research: Biogeosciences, 117 (2012), p. G02018, 10.1029/2011JG001712

Kaiser et al., 2011

M. Kaiser, K. Walter, R.H. Ellerbrock, M. Sommer**Effects of land use and mineral characteristics on the organic carbon content, and the amount and composition of Na-pyrophosphate-soluble organic matter, in subsurface soils**

European Journal of Soil Science, 62 (2011), pp. 226-236

Kaiser et al., 2016

M. Kaiser, D.P. Zederer, R.H. Ellerbrock, M. Sommer, B.Ludwig**Effects of mineral characteristics on content, composition, and stability of organic matter fractions separated from seven forest topsoils of different pedogenesis**

Geoderma, 263 (2016), pp. 1-7

Kim et al., 2003

S. Kim, R.W. Kramer, P.G. Hatcher**Graphical method for analysis of ultrahigh-resolution broadband mass spectra of natural organic matter, the van Krevelen diagram**

Analytical Chemistry, 20 (2003), pp. 5336-5344

Kleber, 2010

M. Kleber**What is recalcitrant soil organic matter?**

Environmental Chemistry, 7 (2010), pp. 320-332

Kleber et al., 2011

M. Kleber, P.S. Nico, A. Plante, T. Filley, M. Kramer, C.Swanston, P. Sollins**Old and stable soil organic matter is not necessarily chemically recalcitrant: implications for modeling concepts and temperature sensitivity**

Global Change Biology, 17 (2011), pp. 1097-1107

Knicker et al., 2006

H. Knicker, G. Almendros, F.J. González-Vila, J.A.González-Pérez, O. Polvill o**Characteristic alterations of quantity and quality of soil organic matter caused by forest fires in continental Mediterranean ecosystems: a solid-state 13C NMR study**

European Journal of Soil Science, 57 (2006), pp. 558-569

Knorr, 2013

K.H. Knorr**DOC-dynamics in a small headwater catchment as driven by redox fluctuations and hydrological flow paths – are DOC exports mediated by iron reduction/oxidation cycles?**

Biogeosciences, 10 (2013), pp. 891-904

Kögel-Knabner, 2000

I. Kögel-Knabner**Analytical approaches for characterizing soil organic matter**

Organic Geochemistry, 31 (2000), pp. 609-625

Komlos et al., 2008

J. Komlos, A. Peacock, R.K. Kukkadapu, P.R. Jaffé**Long-term dynamics of uranium reduction/reoxidation under low sulfate conditions**

Geochimica et Cosmochimica Acta, 72 (2008), pp. 3603-3615

Kujawinski and Behn, 2006

E.B. Kujawinski, M.D. Behn**Automated analysis of electrospray ionization Fourier transform ion cyclotron resonance mass spectra of natural organic matter**

Analytical Chemistry, 78 (2006), pp. 4363-4373

Lalonde et al., 2012

K. Lalonde, A. Mucci, A. Ouellet, Y. Gelinas**Preservation of organic matter in sediments promoted by iron**

Nature, 483 (2012), pp. 198-200

Lehmann et al., 2007

J. Lehmann, J. Kinyangi, D. Solomon**Organic matter stabilization in soil microaggregates: implications from spatial heterogeneity of organic carbon contents and carbon forms**

Biogeochemistry, 85 (2007), pp. 45-57

Loeppert and Inskeep, 1996

R.H. Loeppert, W.P. Inskeep**Iron**

D.L. Sparks (Ed.), Methods of Soil Analysis. Part 3. Chemical Methods, ASA and SSSA, Madison, WI (1996), pp. 639-664

Lopez-Sangil and Rovira, 2013

L. Lopez-Sangil, P. Rovira**Sequential chemical extractions of the mineral-associated soil organic matter: an integrated approach for the fractionation of organo-mineral complexes**

Soil Biology and Biochemistry, 62 (2013), pp. 57-67

Masiello et al., 2004

C.A. Masiello, O.A. Chadwick, J. Southon, M.S. Torn, J.W. Harden**Weathering controls on mechanisms of carbon storage in grassland soils**

Global Biogeochemical Cycles, 18 (2004), p. GB4023

Minor et al., 2012

E.C. Minor, C.J. Steinbring, K. Longnecker, E.B.Kujawinski**Characterization of dissolved organic matter in Lake Superior and its watershed using ultrahigh resolution mass spectrometry**

Organic Geochemistry, 43 (2012), pp. 1-11

Ohno et al., 2014

T. Ohno, T.B. Parr, M.C.I. Gruselle, I.J. Fernandez, R.L.Sleighter, P.G. Hatcher **Molecular composition and biodegradability of soil organic matter: a case study comparing two new england forest types**

Environmental Science & Technology, 48 (2014), pp. 7229-7236

Pansu and Gautheyrou, 2006

Pansu, M., Gautheyrou, J., 2006. Mineralogical Separation by Selective Dissolution, Handbook of Soil Analysis: Mineralogical, Organic, and Inorganic Methods, pp. 167-219.

Piccolo, 2001

A. Piccolo**The supramolecular structure of humic substances**

Soil Science, 166 (2001), pp. 810-832

Posner, 1966

A.M. Posner**The humic acids extracted by various reagents from a soil**

Journal of Soil Science, 17 (1966), pp. 65-78

Plante et al., 2009

A.F. Plante, J.M. Fernández, J. Leifeld**Application of thermal analysis techniques in soil science**

Geoderma, 153 (2009), pp. 1-10

Poulin et al., 2014

B.A. Poulin, J.N. Ryan, G.R. Aiken**Effects of iron on optical properties of dissolved organic matter**

Environmental Science & Technology, 48 (2014), pp. 10098-10106

Ramnarine et al., 2011

R. Ramnarine, R. Voroney, C. Wagner-Riddle, K.Dunfield**Carbonate removal by acid fumigation for measuring the $\delta^{13}C$ of soil organic carbon**

Canadian Journal of Soil Science, 91 (2011), pp. 247-250

Reemtsma, 2009

T. Reemtsma**Determination of molecular formulas of natural organic matter molecules by (ultra-) high-resolution mass spectrometry: status and needs**

Journal of Chromatography A, 1216 (2009), pp. 3687-3701

Remusat et al., 2012

L. Remusat, P.-J. Hatton, P.S. Nico, B. Zeller, M.Kleber, D. Derrien**NanoSIMS study of organic matter associated with soil aggregates: advantages, limitations, and combination with STXM**

Environmental Science & Technology, 46 (2012), pp. 3943-3949

Rumpel and Kögel-Knabner, 2011

C. Rumpel, I. Kögel-Knabner**Deep soil organic matter—a key but poorly understood component of terrestrial C cycle**

Plant and Soil, 338 (2011), pp. 143-158

Schmidt et al., 2011

M.W.I. Schmidt, M.S. Torn, S. Abiven, R. Dittmar, G.Guggenberger, I.A. Janssens, M. Kleber, I. Kogel-Knaber, J.Lehmann, D.A.C. Manning, P. Nannipieri, D.P. Rasse, S. Weiner, S.E. Trumbore**Persistence of soil organic matter as an ecosystem property**

Nature, 478 (2011), pp. 49-56

Smith et al., 2008

P. Smith, C. Fang, J.J.C. Dawson, J.B. Moncrieff**Impact of Global Warming on Soil Organic Carbon, Advances in Agronomy**

Academic Press (2008), pp. 1-43

Solomon et al., 2005

D. Solomon, J. Lehmann, J. Kinyangi, B. Liang, T.Schäfer**Carbon K-edge NEXAFS and FTIR-ATR spectroscopic investigation of organic carbon speciation in soils**

Soil Science Society of America Journal, 69 (2005), pp. 107-119

Stevenson, 1994

F.J. Stevenson**Humus Chemistry: Genesis, Composition, Reactions**

John Wiley & Sons (1994)

Stuiver and Polach, 1977

M. Stuiver, H.A. Polach**Discussion reporting of ^{14}C data**

Radiocarbon, 19 (1977), pp. 355-363

Sutton and Sposito, 2005

R. Sutton, G. Sposito**Molecular structure in soil humic substances: the new view**

Environmental Science & Technology, 39 (2005), pp. 9009-9015

Tfaily et al., 2015

M.M. Tfaily, R.K. Chu, N. Tolić, K.M. Roscioli, C.R.Anderton, L. Paša-Tolić, E.W. Robinson, N.J. Hess**Advanced solvent based methods for molecular characterization of soil organic matter by high-resolution mass spectrometry**

Analytical Chemistry, 87 (2015), pp. 5206-5215

Trumbore et al., 1995

S.E. Trumbore, E.A. Davidson, P. Barbosa de Camargo, D.C. Nepstad, L.A. Martinelli**Belowground cycling of carbon in forests and pastures of eastern Amazonia**

Global Biogeochemical Cycles, 9 (1995), pp. 515-528

Wagai and Mayer, 2007

R. Wagai, L.M. Mayer**Sorptive stabilization of organic matter in soils by hydrous iron oxides**

Geochimica et Cosmochimica Acta, 71 (2007), pp. 25-35

Wagai et al., 2013

R. Wagai, L.M. Mayer, K. Kitayama, Y. Shirato**Association of organic matter with iron and aluminum across a range of soils determined via selective dissolution techniques coupled with dissolved nitrogen analysis**

Biogeochemistry, 112 (2013), pp. 95-109

Wattel-Koekkoek et al., 2001

E.J.W. Wattel-Koekkoek, P.P.L. van Genuchten, P. Buurman, B. van Lagen**Amount and composition of clay-associated soil organic matter in a range of kaolinitic and smectitic soils**

Geoderma, 99 (2001), pp. 27-49

Weishaar et al., 2003

J.L. Weishaar, G.R. Aiken, B.A. Bergamaschi, M.S.Fram, R. Fujii, K. Mopper**Eva luation of specific ultraviolet absorbance as an indicator of the chemical composition and reactivity of dissolved organic carbon**

Environmental Science & Technology, 37 (2003), pp. 4702-4708

Yabusaki et al., 2007

S.B. Yabusaki, Y. Fang, P.E. Long, C.T. Resch, A.D.Peacock, J. Komlos, P.R. Jaffe, S.J. Morrison, R.D. Dayvault, D.C.White, R.T. Anderson**Uranium removal from groundwater via in situ biostimulation: field-scale modeling of transport and biological processes**

Journal of Contaminant Hydrology, 93 (2007), pp. 216-235